ISBN: 978-3-95450-219-6 ISSN: 2226-0366 doi: 10.18429/JACoW-LINAC2024-TUPB045

DESIGN UPDATE OF THE POWER COUPLERS FOR THE SINGLE-SPOKE RESONATORS IN INSTITUTE FOR RARE ISOTOPE SCIENCE

J. Yoon*, Y.-W. Jo, Y. Jung, Y.-K. Kim
Institute for Rare Isotope Science, Daejeon, Republic of Korea
D. Cha, D.-K. Lee, Vitzro Nextech Co., Ltd., Ansan, Republic of Korea

Abstract

A heavy-ion accelerator facility was constructed for the Rare Isotope Science Project (RISP) at the Institute for Rare Isotope Science (IRIS) in Daejeon, Korea. A cryomodule with quarter-wave resonators (QWRs) and half-wave resonators (HWRs) was installed in the SCL (Superconducting Linac) 3 tunnel, and the initial beam commissioning using argon beams has been completed. Additionally, a cryomodule with single-spoke resonators (SSRs), power couplers, and tuners is currently under development for the SCL2 project. The geometry of the fundamental power couplers (FPCs) for the SSRs is a coaxial capacitive type based on a conventional 3-1/8 inch Electronic Industries Alliance (EIA) 50 Ω coaxial transmission line with a single ceramic window. A multi-physics analysis, incorporating electromagnetic, thermal, and mechanical aspects, was conducted to evaluate the design of the power coupler for the SSRs. This paper presents the results of the multi-physics analysis and the current design status of the power coupler for the SSRs.

INTRODUCTION

SCL2 consists of two cavity types, SSR1 and SSR2, with a resonant frequency of 325 MHz. The difference between SSR1 and SSR2 is the ratio of the particle's velocity to the speed of light, denoted as $\beta = v/c$, with values of 0.3 and 0.51, respectively. Additionally, the accelerating voltage differs, being 2.35 MV for SSR1 and 4.2 MV for SSR2. While the fundamental power coupler (FPC) for each cavity type must have different design characteristics, the FPC design for SSR1 and SSR2 can be the same due to their resonant frequency of 325 MHz; the main differences of the FPC are the required power and optimum external quality factor. In this study, we present the updated design of the FPC for 325 MHz SSRs at IRIS. The main parameters are listed in Table 1.

Table 1: Main Parameters of the FPC

Parameter	Value
Operating frequency	325 MHz
Reflection coefficient (FPC only at 325 MHz)	< -20 dB
Operating power (Nominal)	3 kW
Operating power (SSPA)	7 kW
Optimum external quality factor	5.2 $\times 10^6$
Impedance of the vacuum section	90 Ω
Impedance of the air section	50 Ω

* foryjy12@ibs.re.kr

DESIGN UPDATE

To minimize the emission of electrons, the impedance had to be increased, which consequently reduced the diameter of the antenna (vacuum section) compared to a conventional $3\frac{1}{8}$-inch Electronic Industries Alliance (EIA) 50-Ω coaxial transmission line (TL). Figure 1 shows the difference between the previous design and the updated design.

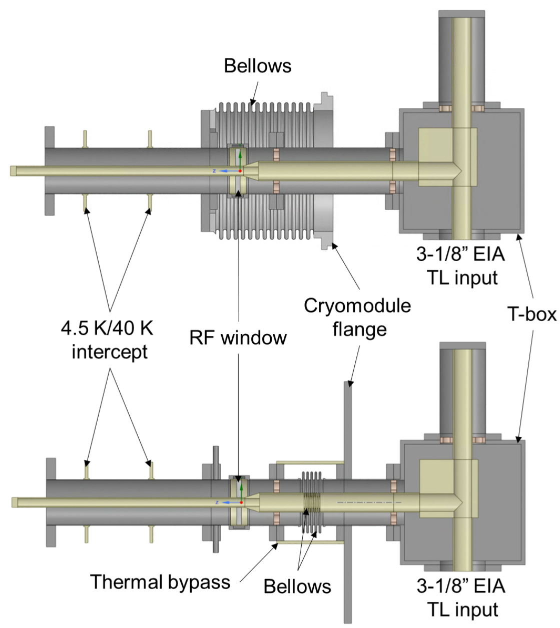

Figure 1: (top) Previous design and (bottom) updated design.

Since the dimensions of the inner conductor are the same in both cases, the results of the electromagnetic field analysis are also identical. The outer conductors are plated with 10 µm of copper, approximately three times the skin depth ($\delta_{Cu,325MHz}$ = 3.62 µm). The T-box allows the supply of RF power to the power coupler via a coaxial transmission line and includes an inner conductor cooling line. The updated design features bellow on the outer and inner conductors within the cryomodule to protect the RF window from mechanical overload [1, 2].

This design allows for the addition of three pick-up ports to monitor arc discharge, electronic emission, and vacuum level variations, which helps prevent RF window breakage. To avoid dew point conditions on the RF window, two Kapton film heaters (maximum 25 W) are attached to the outer conductor on the RF window section to maintain room temperature.

ISBN: 978-3-95450-219-6 ISSN: 2226-0366 doi: 10.18429/JACoW-LINAC2024-TUPB045

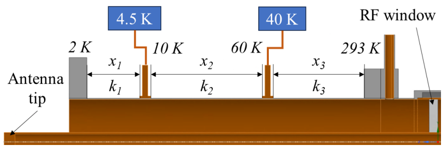

Figure 2: Schematic diagram of the location of the thermal intercepts.

MULTI-PHYSICS ANALYSIS

Thermal Analysis

The power coupler bridges room temperature (300 K) and cryogenic temperature (2 K) and acts as a continuous heat source for the superconducting cavities, as shown in Fig. 2. The thermal intercepts are connected to the liquid helium supply line (4.5 K) and return line (40 K) using copper braided lines. Consequently, the temperature of the intercepts increases to 10 K and 60 K, respectively. The optimal locations of the thermal intercepts were chosen to minimize the static heat loads and were calculated using equations

$$Q_{4.5K,eqv} = 3.0Q_{2K} + Q_{4.5K} + 0.1Q_{40K} \quad (1)$$

and

$$Q_{nK} = \left(A_{Cu}\int k_{Cu}(T)\,dT + A_{STS}\int k_{STS}(T)\,dT\right)/x \quad (2)$$

where Q_{nK} is heat loads to each thermal intercept [3]. $\int k(T)\,dT$ is thermal integrals and A is the area of each materials. The parameters for the heat load calculation are listed in Table 2 [4].

Table 2: Parameters for the Heat Load Calculation

Temperature difference [K]	Thermal integrals [W/mm] Cu (RRR=30)	STS
293 → 60	98.6	2.8
60 → 10	36.2	0.2
10 → 2	2.2	3.2×10^{-3}

Figure 3 shows the 4.5 K equivalent heat load ($Q_{4.5K,eqv}$) variation by the location of the thermal intercepts. We chose the locations of the thermal intercepts as x_1 = 47.8 mm, x_2 = 101 mm, and x_3 = 82.4 mm, which minimize the equivalent heat load to 2.77 W.

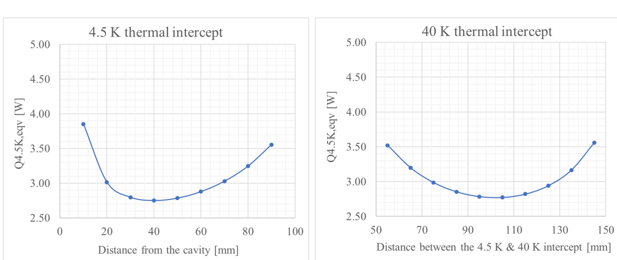

Figure 3: Heat load variation by the intercept locations.

We performed a thermal analysis to evaluate the updated design. Before RF power is applied, the temperature of the RF window is lower than 273 K, which can cause condensation and cold leaks. Therefore, we applied a heater with a power range of 1.4 to 4.1 W to increase the temperature of the window to room temperature. The boundary conditions and results of the thermal analysis are shown in Figs. 4 and 5. The outside of the cryomodule is set with a convection boundary condition, with a heat transfer coefficient of 5 W/m^2·K, representing natural convection. We applied radiation on the copper antenna tip with an emissivity of 0.03 and an ambient temperature of 2 K, corresponding to the operating temperature of the superconducting cavity.

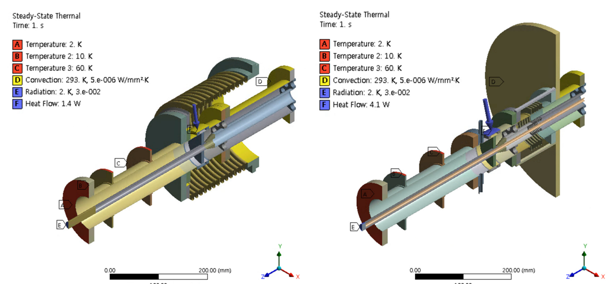
Figure 4: Boundary conditions of the FPC under 0 kW RF power: (Left) previous design and (Right) updated design.

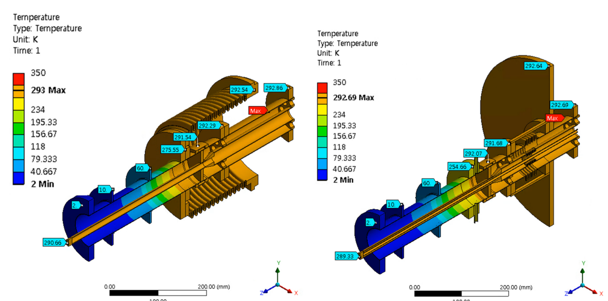
Figure 5: Temperature variations of the FPC under 0 kW RF power: (Left) previous design and (Right) updated design.

The RF losses were calculated using heat flux data from CST Studio Suite, followed by importing into ANSYS Workbench [5, 6]. Thermal results for RF power levels ranging from 0 to 7 kW are listed in Table 3 and shown in Fig. 6. The interlock temperature for the RF window is set at 308 K [7]. In the previous design, the temperature at the RF window exceeds this interlock temperature, with the maximum temperature occurring at the Teflon anchor.

Table 3: Temperature and 4.5 K Equivalent Heat Load Variations by the Applied RF Power

	Previous design		Updated design	
	0 W	7 kW	0 W	7 kW
RF Window	291.5 K	313.5 K	292.1 K	295.3 K
Antenna tip	290.7 K	319.4 K	289.3 K	300.0 K
Teflon	293 K	335.2 K	292.7 K	334.3 K
$Q_{4.5K,eqv}$	2.52 W	2.85 W	2.41 W	2.69 W

ISBN: 978-3-95450-219-6 ISSN: 2226-0366 doi: 10.18429/JACoW-LINAC2024-TUPB045

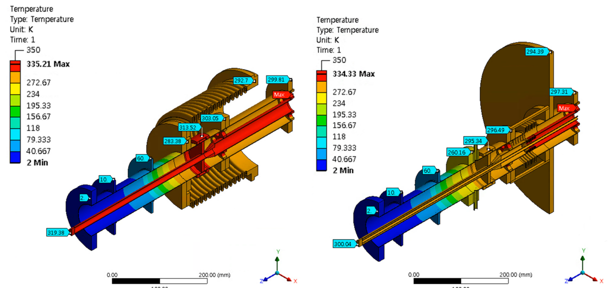
Figure 6: Temperature variations of the FPC under 7 kW RF power: (Left) Previous design and (Right) Updated design.

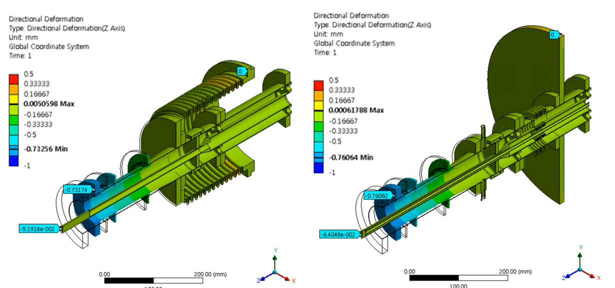
Figure 7: Thermal expansion of the FPC under 0 kW RF power: (Left) previous design and (Right) updated design.

Mechanical Analysis

Before RF power is applied, the FPC contracts due to the low temperature, as shown in Fig. 7. When RF power is subsequently applied, the temperature of the FPC increases, leading to thermal expansion. We performed a mechanical analysis to check the length variation of the flange connecting with the cavity flange and the antenna tip. The results of this analysis are presented in Fig. 8 and detailed in Table 4.

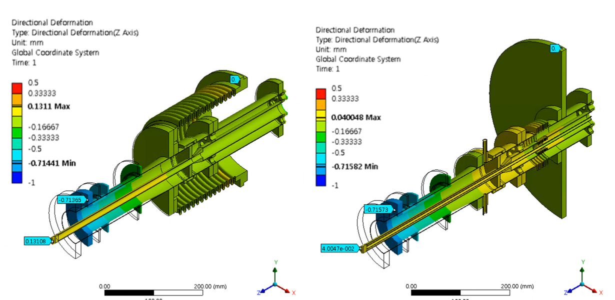
Figure 8: Thermal expansion of the FPC under 7 kW RF power: (Left) previous design and (Right) updated design.

The fixed point is set to the cryomodule flange. The length variations of the flange for each FPC design can be negligible, resulting in 18.0 µm and 44.5 µm, respectively. For the antenna tip, the changes are 183.0 µm and 104.2 µm. The variation in antenna penetration depth affects the optimum external quality factor. The required power variation of the FPC due to changes in the antenna penetration depth is 300 W/mm. Therefore, the required power change for the two cases is 54.9 W and 31.2 W, respectively.

Table 4: Length Variation by the Applied RF Power

	Previous design		**Updated design**	
	0 W	**7 kW**	**0 W**	**7 kW**
Flange	-731.7 µm	-713.7 µm	-760.2 µm	-715.7 µm
Antenna tip	-51.9 µm	131.1 µm	-64.1 µm	40.1 µm

CONCLUSION

We updated the design of the FPC for 325 MHz SSRs and performed a multi-physics analysis. In the traveling wave (TW) and continuous wave (CW) modes, the temperatures of the RF window and antenna tip are below 300 K, with temperature differences of less than 11 K, even at double the operating power. We will conduct thermal and mechanical analysis in standing and continuous wave modes, including air cooling at the inner conductor. Additionally, we will fabricate the updated FPC design and perform high-power and horizontal tests with the cavity and cryomodule by the end of 2025.

ACKNOWLEDGEMENTS

This research received support from the National Research Foundation of Korea (NRF) and was funded by the Ministry of Science and ICT under grants (2013M7A1A1075764) and (RS-2022-00214790).

REFERENCES

[1] V. Zvyagintsev *et al.*, "Fundamental power coupler design for a 325 MHz Balloon SSR Cavity", in *Proc. 19th Int. Conf. on RF Superconductivity (SRF2019)*, Dresden, Germany, July 2019, pp. 252-254. `doi:10.18429/JACoW-SRF2019-MOP076`

[2] S. Kazokov *et al.*, "Latest progress in design and testing of PIP-II power couplers", in *Proc. 19th Int. Conf. on RF Superconductivity (SRF2019)*, Dresden, Germany, July. 2019, pp.263-266. `doi:10.18429/JACoW-SRF2019-MOP080`

[3] T. Huang *et al.*, "Recent progress of FPCs at IHEP", Presented at the 3rd WWFPC Mini-workshop, Geneva, Switzerland, 2017. `https://indico.cern.ch/event/642503/contributions/2638465/attachments/1483543/2301804/Recent_process_of_FPCs_at_IHEP_-_3rd_WWFPC.pdf`

[4] P. Duthil, "Material properties at low temperature", presented at CAS-CERN Accelerator School: Superconductivity for Accelerators, Erice, Italy, April, 2013. `https://cds.cern.ch/record/1973682/files/CERN-2014-005-p77.pdf`

[5] Dssault Systems, CST Studio Suite 2014, `https://www.cst.com`

[6] ANSYS, ANSYS R17.1, `https://www.ansys.com`

[7] Zeqin Yao, *et al*, "High power conditioning of RF couplers for the BISOL Linac", *J. NIM-A*, vol. 1045, p. 167511, 2023. `doi:10.1016/j.nima.2022.167511.`